

Structural Information on the Transition Moments in Poly(ethylene-2,6-naphthalene) by Polarization FT-IR Spectroscopy

Alex Scott,¹ Chady Hakme,² Isabelle Stevenson,² Alison Voice^{*1}

Summary: Oriented poly(ethylene-2,6-naphthalate) (PEN) has been characterised by polarised FT-IR spectroscopy to determine the structural angles of the transition moments to the molecular chain axis. The bands at 1130 cm^{-1} , 1142 cm^{-1} and 1602 cm^{-1} , which have been previously assigned as having their transition dipole moments parallel to the chain axis, are confirmed as parallel bands. Bands at 767 cm^{-1} and 831 cm^{-1} are confirmed as perpendicular bands. However the band at 1708 cm^{-1} which has previously been assigned as a perpendicular band, is shown here to have its transition moment at 72° to the molecular axis.

Keywords: FT-IR; molecular orientation; poly(ethylene-2,6-naphthalate); refractive index; uniaxial

Introduction

Poly(ethylene-2,6-naphthalate) (PEN) receives industrial interest as one of a number of high performance polymers. The naphthalene ring in the PEN repeat unit (Figure 1) is thought to give greater rigidity to the macromolecular chain and hence superior mechanical properties relative to other closely related polymers. In comparison with poly(ethylene terephthalate) (PET), PEN has a higher mechanical strength, higher melting point (270°C , compared with 255°C for PET) and better hydrolytic resistance. PEN has a relatively high glass transition temperature ($T_g \approx 120^\circ\text{C}$)^[1–5] compared with $\sim 72^\circ\text{C}$ for PET.^[1] Such properties of PEN favour its use in applications such as capacitor dielectrics, data storage tapes, packaging, e-paper and flexible OLEDs.

The purpose of the work described here is to determine the angles that the IR dipole transition moments make relative to the

macromolecular backbone of the PEN chain. Although several research teams have assigned the various peaks in the IR spectrum of PEN to specific molecular vibrational modes,^[6,7] the direction of these moments have not been determined. Knowledge of these angles would significantly reduce the time needed to obtain a quantitative analysis of molecular orientation of PEN films, since it could then be determined from IR spectroscopy alone.

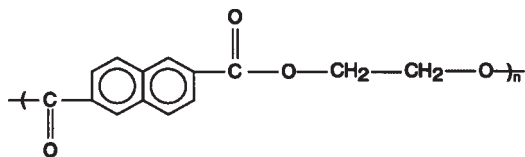
Theory

A quantitative analysis of the orientation of the molecular chains within a uniaxially drawn polymer can be obtained from polarised IR spectroscopy alone providing the structural details of the transition moments are known. Conversely if the orientation function can be obtained from some other experimental method (e.g. birefringence) then the angles that the transition moments make with the molecular chain can be determined by combining the IR and birefringence data.

A uniaxial distribution is characterised by one single axis, namely the draw

¹ IRC in Polymer Science & Technology, School of Physics & Astronomy, University of Leeds, Leeds, LS2 9JT, UK

² Laboratoire des Matériaux Polymères et des Biomatériaux, UMR CNRS 5627, Bât. ISTIL; 43, Bld du 11 novembre 1918; 69622 Villeurbanne Cedex, France

**Figure 1.**

Structural diagram of the repeat unit in PEN.

direction (Figure 2), and the orientation average, $\langle P_2(\cos \theta) \rangle$ of the molecular chain axes to the draw direction can be determined from birefringence measurements. This involves measuring the birefringence ($\Delta n = n_3 - n_1$) of the separate orthogonal refractive indices, and also requires knowledge of the intrinsic birefringence, Δn_0 , of the polymer concerned. $\langle P_2(\cos \theta) \rangle$ is then determined from equation 1.

$$\langle P_2(\cos \theta) \rangle = \frac{\Delta n}{\Delta n_0} = \frac{n_3 - n_1}{\Delta n_0} \quad (1)$$

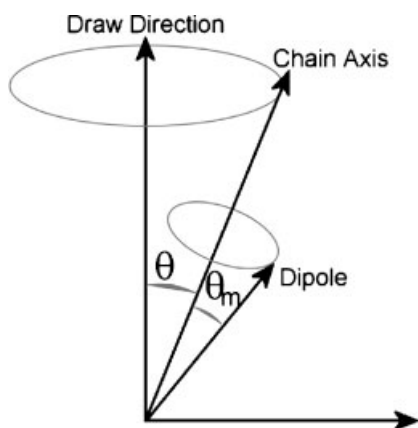
For thin films directions 1, 2 and 3 are defined within the drawn sample such that the refractive index n_3 is parallel to the draw direction, n_2 is normal to the film plane and n_1 is within the film plane but normal to the draw direction (Figure 3).

If it is assumed that each IR-active vibrational mode has its transition moment at a well defined angle (θ_m) to the molecular

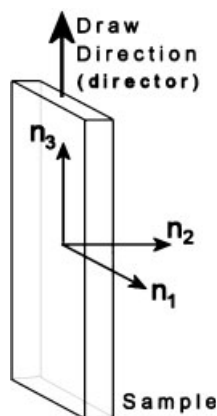
chain axis and that these transition moments are distributed uniaxially about the chain axes then polarised IR spectroscopy can be used to determine these angles via equation 2,3 and 4.

Two IR spectra are obtained for each drawn film (films drawn to a range of draw ratios). For each film one spectrum is obtained with the IR radiation polarised parallel to the draw direction and one with it polarised perpendicular to the draw direction. For each peak in the spectrum (i.e. for each transition moment) the areas $A_{//}$ and A_{\perp} (being the areas in the parallel and perpendicular spectra respectively) are determined and combined via equation 2 to yield the orientation average of the transition moments with respect to the draw direction, $\langle P_2(\cos \theta_\mu) \rangle$ where θ_μ is the angle between the transition moment (dipole) and the draw direction.

$$\langle P_2(\cos \theta_\mu) \rangle = \frac{A_{//} - A_{\perp}}{A_{//} + 2A_{\perp}} \quad (2)$$

**Figure 2.**

Angles considered in the study of uniaxially drawn films.

**Figure 3.**

Directions of the three refractive indices in the sample.

The angle of each transition moment to the molecular chain, θ_m , is obtained via equation 3 by fitting a straight line to a graph of $\langle P_2(\cos \theta_\mu) \rangle$ against $\langle P_2(\cos \theta) \rangle$ for samples drawn to different draw ratios. The slope of this line $\langle P_2(\cos \theta_m) \rangle$ is then used in equation 4 for the Hermans orientation function, to obtain θ_m

$$\langle P_2(\cos \theta_m) \rangle = \frac{\langle P_2(\cos \theta_\mu) \rangle}{\langle P_2(\cos \theta) \rangle} \quad (3)$$

$$\langle P_2(\cos \theta_m) \rangle = \frac{1}{2}(3 \cos^2 \theta_m - 1) \quad (4)$$

Materials

PEN film (nominally 45 μm thick, amorphous and isotropic) was supplied by DuPont Teijin Films Ltd. (Luxemburg). Samples (approximately 75 mm long by 20 mm wide) were cut from this film. Care was taken to avoid any fraying along the cut edges so as not to introduce weaknesses which may cause undesirable drawing or breaking of the samples.

Uniaxial Drawing

Drawing was carried out using an Instron 4505 tensile testing machine at a temperature of $150 \pm 3^\circ\text{C}$ and speed of 500 mm/min. This produced a range of samples (with draw ratios between 3.6 and 6.1) which were reasonably transparent and hence suitable for optical experiments.

All samples exhibited necking during the drawing process which means that a neck is initiated in the film and travels down the length of the sample producing drawn material at the 'natural' draw ratio. For PEN this natural draw ratio was found to be approximately 3.6, where draw ratio, λ , is defined as the quotient of final length of a sample and its original length. Producing samples of higher draw ratio can only be achieved once the neck has extended over the whole length of the sample. However producing samples of lower draw ratio can only be achieved if conditions can be found under which the necking phenomenon is not observed. Samples drawn at 85°C were

found to draw reasonably evenly and a sample of draw ratio 2.0 was obtained in this way. However it should be noted that this sample has been drawn below T_g (all others are drawn above T_g) and it will not be included in discussions of trends with draw ratio, although it is included in the analysis to determine transition moment angles.

To determine the draw ratio of each sample dots were marked on the undrawn film at 2 mm intervals. After each sample had been drawn, a region over which drawing appeared even was analysed and the length of this region measured from one dot to another, and scaled by the separation of these dots.

Polarization Spectroscopy

Infrared spectra were taken using a Bomem FT-IR Spectrometer over the range 200–5000 cm^{-1} with resolution 4 cm^{-1} . A reference scan was taken at the beginning of each session which was subsequently subtracted from each sample spectrum. Each spectrum (including the reference spectrum) was built up over 100 scans. To prevent absorption of infrared radiation due to water vapour and carbon dioxide, the sample chamber was purged with dry nitrogen. To obtain the two polarised spectra the sample draw direction was mounted parallel, and then perpendicular to the pass direction of the polariser. The polariser itself remained in a fixed orientation to avoid any polarisation sensitivity of the optics within the spectrometer.

Before any peak fitting was carried out a linear baseline correction was applied to the data using the GRAMS32 software. Peak fitting was then undertaken using the GRAMS32 package in the range from 700–3200 cm^{-1} , allowing all peaks to be considered as a mixture of Gaussian and Lorentzian lineshapes. This was done with reference to assignments made by Ouchi et al.^[6] The difference between the sum of the fitted peaks and the spectrum was minimised using a least squares residual optimisation procedure. Finally, when suitable fitted spectra had been obtained the

areas of the fitted peaks were tabulated against wavenumber for each draw ratio and $\langle P_2 \cos \theta_\mu \rangle$ was evaluated according to equation 2 for each band at all draw ratios.

Compensation Microscopy

A compensating microscope was used to measure the birefringence ($\Delta n = n_3 - n_1$) of all samples.^[8] A white light source was used in order that the zeroth order fringe could be identified.

Literature by Orchard and Ward,^[9] Voice et al.^[8] and Faust and Marrinan^[10] suggests that for samples of high birefringence the phenomenon of fringe jumping may be encountered, and this was indeed found to be the case with PEN. Fringe jumping arises due to the differing dispersions of the sample and the compensator. This causes the black fringe to be observed in a position which does not correspond to the zeroth order. To overcome the problem of fringe jumping it is possible to scan across a sample from a region of low birefringence to the region where the measurement of birefringence is needed. The position of the zeroth order fringe can thus be tracked and its true position determined. This allows a graph of apparent fringe number versus true fringe number to be plotted, the slope of which was determined to be 1.159 for these PEN samples. However only 3 points could be obtained for this graph due to a lack of suitable samples.

Refractometry

To determine the 3 mutually orthogonal refractive indices separately an Abbe Refractometer was used with sodium light source at a wavelength of 589.3 nm. To ensure good optical contact a coupling liquid was employed, which had a higher refractive index than the sample and a lower refractive index than the prism to ensure light entered the prism. This method allowed n_1 and n_2 (Figure 3) to be determined. However n_3 was only able to be determined directly for samples of very low draw ratio, since for samples of higher draw ratio n_3 was found to be greater than

the refractive index of the prism in the refractometer.

Differential Scanning Calorimetry

DSC measurements were carried out using a 2920 TA Instruments device in the temperature range from 30 °C to 300 °C using a heating rate of 10 °C /min. Sample weights were around 4 mg. Samples consisting of a flat single layer film were used to reduce heat flow lags. Baseline calibration was undertaken using indium. All samples were sealed in aluminium pans and the measurements were performed under a high purity helium atmosphere. The degree of crystallinity was calculated using the crystallization enthalpy of 190 J/g measured for a 100% crystalline PEN.^[11]

Results and Discussion

Undrawn Material

For the undrawn sample ($\lambda = 1$) the refractive indices, n_1 , n_2 and n_3 , were found to be identical within the uncertainties, confirming that the original PEN film supplied by DuPont was isotropic (Table 1). This is also confirmed by the low measured birefringence. The mean refractive index of the undrawn film was found to be 1.647 and Miyata et al.^[12] report similar a value; $n = 1.65$.

The DSC heat flow curve of the undrawn PEN (Figure 4) shows a T_g at about 120 °C followed by cold crystallization at $T_c = 188$ °C and melting at $T_m = 268$ °C. The areas of the crystallisation and melting peaks for this film are identical (within experimental uncertainties) and confirm that the crystallinity of the supplied undrawn PEN is essentially zero.

Development of Crystallinity with

Draw Ratio

The uniaxially drawn PEN films display a sharp melting endotherm with a maximum located at a temperature similar to that of the undrawn sample. The cold crystallization peak disappears completely for all draw ratios higher than 2. It is suggested

Table 1.

Draw ratio, birefringence, refractive indices, $\langle P_2(\cos \theta) \rangle$ from birefringence using $\Delta n_0 = 0.41$ and crystallinity of PEN samples.

λ	Δn	n_1	n_2	n_3	$\langle P_2(\cos \theta) \rangle$	Crystallinity from DSC
1.0	0.001	1.6461	1.645	1.65	0.002	~0
2.0	0.041	1.6148	1.610	1.66	0.100	1.6
3.6	0.234	1.608	1.578		0.571	31.2
3.7	0.217	1.5895	1.579		0.529	31.9
3.9	0.234	1.5968	1.57		0.571	34.2
4.5	0.30	1.589	1.56		0.732	35.4
5.0	0.30	1.5796	1.55		0.732	36.2
5.7	0.29	1.5735	1.549		0.707	37.2
6.1	0.31	1.573	1.547		0.756	38.1

that the orientation induced by stretching triggers the increase of crystallization. As can be seen from Figure 5 the relationship between crystallinity and draw ratio indicates a rapid rise in crystallinity at low draw ratios and a levelling out at $\lambda > 4$.

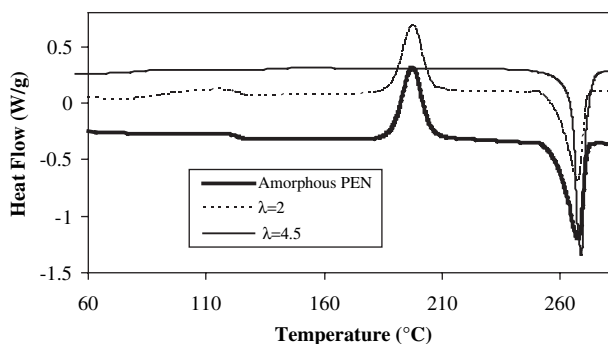
Development of Molecular Orientation with Draw Ratio

Huijits and Peters report in their work^[13] that evidence is provided for the linear relationship between birefringence and molecular orientation and thus equation 1 is assumed a valid method for determining the overall orientation of the films.

To determine the average molecular orientation of the drawn films from equation 1 requires knowledge of the intrinsic birefringence of PEN. Several values are available in the literature. Huijits and Peters^[13] have measured the birefringence of PEN samples and extrapolated to estimate the value for perfectly aligned

molecules and quote a value of $\Delta n_0 = 0.487 \pm 0.017$, although they remark that this value is likely to be too high. Carr, Zhang and Ward^[14] have calculated the intrinsic birefringence by summing the bond polarisabilities and quote a value of $\Delta n_0 = 0.332$. However they point out that this value is expected to be an underestimate due to the use of bond polarisability data for a benzene ring in the absence of suitable data for a naphthalene ring. Miyata et al.^[12] report a value of $\Delta n_0 = 0.336$. In the light of this information an average value of $\Delta n_0 = 0.410$ was used in this research.

The refractive indices, n_1 and n_2 , measured using the Abbe refractometer, are expected to be equal to each other for uniaxially drawn films, however, n_2 appears to be slightly lower than n_1 in all cases, nonetheless $(n_1 - n_2) \ll \Delta n$. This result hints at a preferential orientation relative to the sample surfaces. Such an effect is

**Figure 4.**

DSC curves for undrawn and drawn ($\lambda = 2$ and 4.5) films, shifted vertically for clarity.

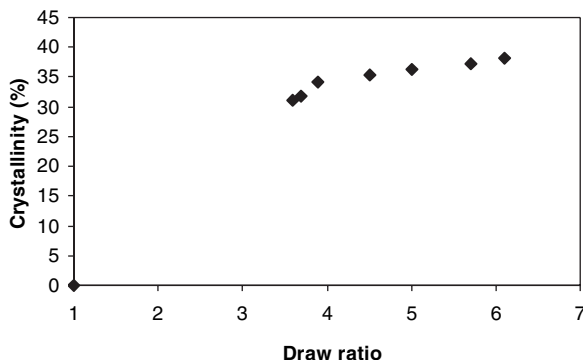


Figure 5.

Crystallinity from DSC versus draw ratio.

noted by Hayashi et al.,^[15] Cakmak and Kim^[16] and Murakami et al.^[17] who all report that the naphthalene plane orients parallel to the broad surface of the film on both uniaxial and biaxial drawing. Thus it is concluded that the drawing process is not strictly uniaxial, but a close enough approximation to it.

A graph of $\langle P_2(\cos \theta) \rangle$ versus draw ratio can be seen in Figure 6. This shows a rapid rise at low draw ratio and a levelling out at draw ratios above 4.5. This suggests that the polymer is drawing according to the pseudo-affine regime^[18] characteristic of semi-crystalline polymers. A comparison of Figures 5 and 6 shows a strong correlation between crystallinity and $\langle P_2(\cos \theta) \rangle$, although when plotted against each other

the data is too clumped to conclude whether the relationship is strictly linear, but it certainly supports this idea.

Development of Orientation of Specific Bands with Draw Ratio

The parallel and perpendicular spectra obtained for the most highly drawn PEN film are shown in Figure 7. The development of $\langle P_2(\cos \theta_\mu) \rangle$, obtained via polarised FT-IR spectroscopy, with increase in draw ratio is shown for selected bands in Table 2.

Determining Transition Moment Angles

For each band considered $\langle P_2(\cos \theta_m) \rangle$ was evaluated using equation 3. A quadratic fit to a graph of $\langle P_2(\cos \theta_\mu) \rangle$ against $\langle P_2(\cos \theta) \rangle$ was used (since not all bands showed linear

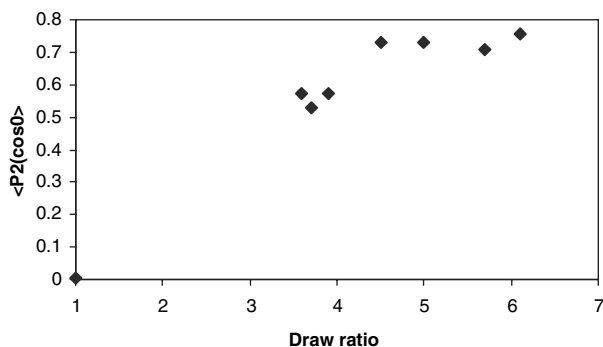


Figure 6.

Graph of $\langle P_2(\cos \theta) \rangle$ against draw ratio.

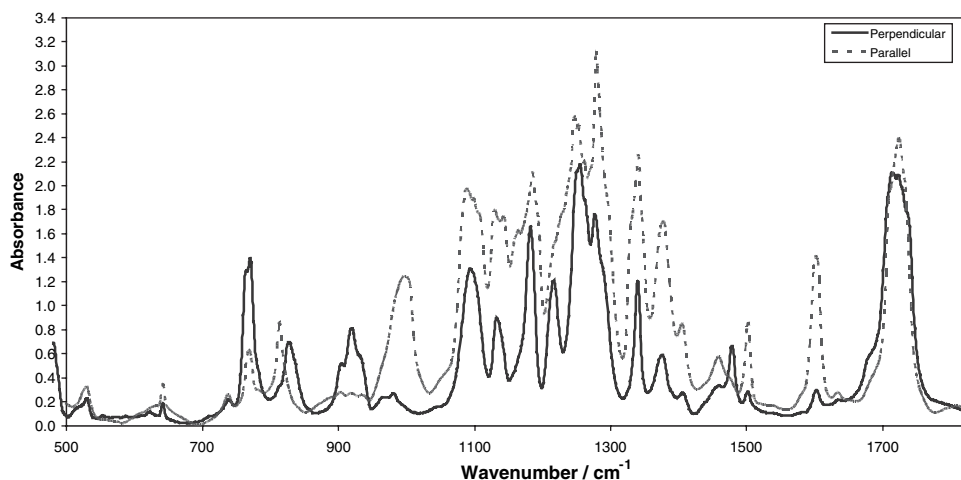


Figure 7.

Parallel and perpendicular spectra for drawn PEN film with draw ratio $\lambda = 6.1$.

behaviour). Four such plots are shown in Figure 8. Equation 4 was then used to evaluate θ_m from the local slope at low orientation ($\langle P_2(\cos \theta) \rangle = 0.01$) and high orientation ($\langle P_2(\cos \theta) \rangle = 0.8$) (Table 3). The choice of Δn_0 has a slight effect on the values of θ_m determined. But using the widest range of published values for Δn_0 affects θ_m by $\pm 5^\circ$.

Conclusions

The first obvious conclusion from Table 3 is that some bands (1047, 1376, 1502 and 1708 cm^{-1}) show a linear relationship between $\langle P_2(\cos \theta_\mu) \rangle$ and $\langle P_2(\cos \theta) \rangle$, and hence have no change of θ_m with overall

molecular orientation. The band at 1602 cm^{-1} can probably also be included in this group since at low angles there exists extreme sensitivity of θ_m to changes in $\langle P_2(\cos \theta_m) \rangle$.

Bands at 767 and 831 cm^{-1} are seen to have transition moment angles approaching 90° as the molecular orientation increases. These two bands were assigned as \perp by Ouchi^[6] and the work here supports this assignment for well oriented films. Further confirmation is provided when the nature of the vibrational assignments are considered; 767 cm^{-1} is attributed to the out of plane bending of the aromatic ring CH groups (positions 3, 4, 5, 6, 7 and 8 in Figure 9) and 831 cm^{-1} is attributed to the rocking of the trans CH_2 units in the aliphatic section of

Table 2.
 $\langle P_2(\cos \theta_\mu) \rangle$ from FT-IR.

λ	767 cm^{-1}	831 cm^{-1}	1047 cm^{-1}	1084 cm^{-1}	1096 cm^{-1}	1130 cm^{-1}	1142 cm^{-1}	1333 cm^{-1}	1376 cm^{-1}	1502 cm^{-1}	1602 cm^{-1}	1708 cm^{-1}
1.0	0.001	-0.021	0.007	0.013	0.002	0.004	0.030	0.010	0.014	0.003	0.004	-0.018
2.0	-0.053	-0.094	0.046	0.059	0.027	0.050	0.024	0.024	0.053	0.070	0.030	-0.035
3.6	-0.145	-0.130	0.177	0.073	0.085	0.085	0.130	0.388	0.331	0.070	0.539	-0.223
3.7	-0.185	-0.232	0.185	0.102	0.130	0.173	0.178	0.403	0.378	0.240	0.545	-0.180
3.9	-0.187	-0.158	0.186	0.087	0.128	0.207	0.200	0.330	0.308	0.246	0.479	-0.222
4.5	-0.209	-0.277	0.211	0.180	0.208	0.288	0.294	0.397	0.452	0.243	0.657	-0.286
5.0	-0.282	-0.309	0.222	0.160	0.135	0.356	0.351	0.364	0.441	0.439	0.643	
5.7	-0.274	-0.277	0.221	0.209	0.216	0.298	0.527	0.401	0.359	0.086	0.910	
6.1	-0.322	-0.322	0.301	0.148	0.214	0.346	0.392	0.469	0.490	0.201	0.687	-0.264

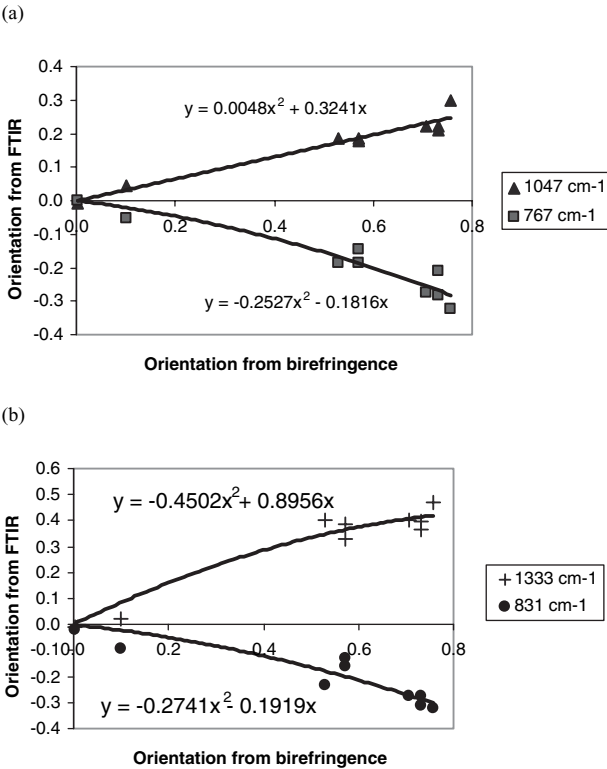


Figure 8. Variation of molecular orientation determined from FT-IR, $\langle P_2(\cos \theta_{\mu}) \rangle$, for four transition moments, plotted against $\langle P_2(\cos \theta) \rangle$ determined from birefringence.

the chain (positions 11 and 12 in Figure 9). Both of these vibrations would intuitively be assigned as perpendicular to the chain axis.

Bands at 1130 and 1142 cm^{-1} exhibit a large change of angle with increasing molecular orientation, although the transition moments become increasingly aligned to

Table 3. Band positions, assignments (as reported by Ouchi et al.^[6]) and the calculated angles of the transition moments with respect to the chain axis, θ_m .

Wavenumber (cm^{-1})	Assignments ^[6]	θ_m ($^\circ$) at low orientation	θ_m ($^\circ$) at high orientation
767	Bending aromatic ring CH out of plane	63	90 ^{a)}
831	Crystal state only and assigned to the rocking of CH ₂ Trans	63	90 ^{a)}
1047	Antisymmetric C–O stretching vibration	42	42
1084	Symmetric C–O stretching vibration	52	38
1096	Symmetric C–O stretching vibration	51	37
1130	Napthalene ring vibration	58	0 ^{b)}
1142	Napthalene ring vibration	63	0 ^{b)}
1333	Wagging in CH ₂ Trans (crystal state formed by heating)	16	48
1376	Wagging in CH ₂ Gauche (crystal state)	31	31
1502	Aromatic ring vibration	40	44
1602	Aromatic ring vibration	17	0 ^{b)}
1708	C=O stretching	73	72

^{a)} θ_m assumed to be 90° despite local gradient slightly >1 due to experimental uncertainty.
^{a)} θ_m assumed to be 0° despite local gradient slightly <–0.5 due to experimental uncertainty.

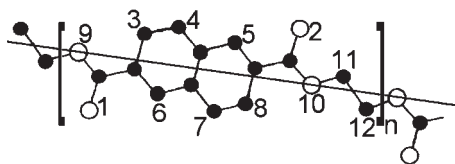


Figure 9.

Schematic representation of the PEN repeat unit (hydrogen atoms not shown). The long straight line represents the molecular chain axis.

the chain axis as the molecular orientation increases. This confirms Ouchi's assignment of the combined band at 1135 cm^{-1} as being 'parallel', even if only for highly oriented films.

The band at 1602 cm^{-1} also confirms Ouchi's assignment of this as a \parallel band. However the band at 1708 cm^{-1} due to the C=O stretching vibration (positions 1 and 2 in Figure 9), which is assigned by Ouchi as a \perp band, is shown in this work to have an angle of 73° to the chain axis, independent of the degree of orientation of the molecules.

Acknowledgements: The authors would like to thank Dr M Bonner, Dr L Saunders, and Dr E Lewis for their advice and help. Thanks are also

due to DuPont Teijin Ltd for supplying the PEN film.

- [1] Ito, Takahashi & Kanamoto, *Polymer* **2002**, 43, 3675.
- [2] Higashioji et al, *Tribology International* **2003**, 36, 437.
- [3] Cakmak & Kim, *Journal of Applied Polymer Science* **1997**, 64, 729.
- [4] Bedia et al, *Polymer* **2001**, 42, 7299.
- [5] DuPont Teijin Films, Teonex Q71 Datasheet.
- [6] Ouchi, Hosoi & Shimotsuma, *Journal of Applied Polymer Science* **1977**, 21, 3445.
- [7] Vasanthan, N. & Salem, D.R. *Macromolecules* **1999**, 32, 6318.
- [8] Voice et al, *Polymer* **1993**, 34, 1154.
- [9] Orchard & Ward, *Polymer* **1992**, 33, 4207.
- [10] Faust & Marrinan, *British Journal of Applied Physics* **1955**, 6, 351.
- [11] S Buchner et al, *Polymer* **1989**, 30, 480.
- [12] Miyata, Kikutani & Okui, *Journal of Applied Polymer Science* **1997**, 65, 1415.
- [13] Huijits & Peters, *Polymer* **1994**, 35, 3119.
- [14] Carr, Zhang & Ward, *Polymers for Advanced Technologies* **1995**, 7, 39.
- [15] Hayashi et al, *Polymer Journal* **1985**, 17, 953.
- [16] Cakmak & Kim, *Polymer Engineering and Science* **1990**, 30, 721.
- [17] Murakami et al, *Polymer* **1995**, 36, 2291.
- [18] Crawford and Kolsky, *Proc. Phys. Soc. B* **1951**, 64, 119.